

Octameric enolase from the hyperthermophilic bacterium *Thermotoga maritima*: Purification, characterization, and image processing*

HARTMUT SCHURIG,¹ KERSTIN RUTKAT,¹ REINHARD RACHEL,²
AND RAINER JAENICKE¹

¹ Institut für Biophysik und Physikalische Biochemie, Universität Regensburg, D-93040 Regensburg, Germany

² Lehrstuhl für Mikrobiologie, Universität Regensburg, D-93040 Regensburg, Germany

(RECEIVED October 7, 1994; ACCEPTED November 17, 1994)

Abstract

Enolase (2-phospho-D-glycerate hydrolase; EC 4.2.1.11) from the hyperthermophilic bacterium *Thermotoga maritima* was purified to homogeneity. The N-terminal 25 amino acids of the enzyme reveal a high degree of similarity to enolases from other sources. As shown by sedimentation analysis and gel-permeation chromatography, the enzyme is a 345-kDa homooctamer with a subunit molecular mass of 48 ± 5 kDa. Electron microscopy and image processing yield ring-shaped particles with a diameter of 17 nm and fourfold symmetry. Averaging of the aligned particles proves the enzyme to be a tetramer of dimers. The enzyme requires divalent cations in the activity assay, Mg^{2+} being most effective. The optimum temperature for catalysis is 90 °C, the temperature dependence yields a nonlinear Arrhenius profile with limiting activation energies of 75 kJ mol⁻¹ and 43 kJ mol⁻¹ at temperatures below and above 45 °C. The pH optimum of the enzyme lies between 7 and 8. The apparent K_m values for 2-phospho-D-glycerate and Mg^{2+} at 75 °C are 0.07 mM and 0.03 mM; with increasing temperature, they are decreased by factors 2 and 30, respectively. Fluoride and phosphate cause competitive inhibition with a K_i of 0.14 mM. The enzyme shows high intrinsic thermal stability, with a thermal transition at 90 and 94 °C in the absence and in the presence of Mg^{2+} .

Keywords: enolase; glycolysis; thermostability; *Thermotoga maritima*

The hyperthermophilic bacterium *Thermotoga maritima* represents one of the deepest branches in the bacterial domain of the phylogenetic tree (Stetter, 1993). The bacterium metabolizes simple and complex carbohydrates using the conventional Embden-Meyerhof-Parnas pathway (Huber et al., 1986; Blamey & Adams, 1994). Under normal growth conditions, a number of glycolytic enzymes are expressed to relatively high levels. Some of them have been purified and characterized in detail: GAPDH (Wrba et al., 1990; Rehder & Jaenicke 1992), LDH (Ostendorp

et al., 1993), PGK, and PGK/TIM fusion protein (Schurig et al., 1995). Here we report the isolation and the gross properties of enolase (2-phospho-D-glycerate hydrolase; EC 4.2.1.11).

The ubiquitous metalloenzyme (Wold, 1971; Brewer, 1981) catalyzes the reversible dehydration of 2-PGA to PEP. Crystallographic studies on yeast apo-enolase (Stec & Lebioda, 1990) showed that the enzyme belongs to the family of α/β -barrel enzymes, like TIM (Farber & Petsko, 1990).

With respect to their state of association, homodimeric and homooctameric enolases have been reported. The homooctameric forms come from organisms of the bacterial domain including two enolases from thermophilic sources (Barnes & Stellwagen, 1973; Stellwagen et al., 1973). Recently, the isolation and characterization of an enolase from the hyperthermophilic archaeon *Pyrococcus furiosus* was reported (Peak et al., 1994). The present work refers to enolase from the hyperthermophile *T. maritima*. This bacterium has become a favorite source of "hyperstable" proteins in connection with attempts to get deeper insight into the evolution and structure-function relationship of proteins at high temperatures (Jaenicke, 1991, 1993).

* This paper is dedicated to Professor John A. Schellman on the occasion of his 70th birthday.

Reprint requests to: Rainer Jaenicke, Institut für Biophysik und Physikalische Biochemie, Universität Regensburg, D-93040 Regensburg, Germany; e-mail: jaenicke.vax1.rz.uni-regensburg.d400.de.

Abbreviations: BCA, bicinechonic acid; GAPDH, glyceraldehyde 3-phosphate dehydrogenase; GdmCl, guanidinium-chloride; HEPES, *N*-2-hydroxyethyl-piperazine-*N'*-2-ethanesulfonic acid; LDH, lactate dehydrogenase; MES, 2-(*N*-morpholino)ethanesulfonic acid; PEP, phosphoenolpyruvate; 2-PGA, 2-phospho-D-glycerate; PGK, phosphoglycerate kinase; TIM, triosephosphate isomerase.

Results

Purification of enolase

Enolase from *T. maritima* was purified from crude cell extracts using standard chromatographic techniques (Table 1). In preparations from different cell charges, we found varying profiles eluting from the Q-Sepharose HP anion-exchange column depending on their DNA content. Complete removal of DNA eliminates the unusual binding behavior so that this purification step becomes reproducible and effective. The purification of the enzyme was followed by SDS-PAGE, as illustrated in Figure 1. In its purified form, the homogeneity of the enzyme exceeded 95%, as taken from silver-stained SDS-PAGE and N-terminal sequencing. The yield of purified enolase was 10–15 mg from 100 g wet cells (50% recovery of total enzymatic activity), with a specific activity of 250 U/mg at 40 °C.

As shown by atomic absorption, the enzyme contains firmly bound magnesium ions. They can be removed by dialysis against EDTA.

N-terminal sequencing

Twenty-five N-terminal amino acid residues of the purified enzyme were sequenced by Edman degradation. The sequence shows high similarity to other enolases from eukaryotic organisms and to the enzyme from the archaeon *P. furiosus* (Fig. 2).

Molecular properties

The molecular mass and the subunit composition were determined by SDS-PAGE, gel-permeation chromatography, and analytical ultracentrifugation. Sedimentation velocity experiments at 0.03–0.2 mg/mL in 100 mM Tris/HCl buffer, pH 7.5, yield single symmetrical boundaries with sedimentation constants $s_{20,w}^0 = 13.7 \pm 0.2$ S in the presence of 2 mM $MgCl_2$, and 13.4 S for the magnesium-free apoenzyme. At acid pH (100 mM glycine/HCl buffer, pH 2.3), the sedimentation coefficient drops to $s_{20,w} = 7.3$ S; GdmCl denaturation (4 M GdmCl, pH 7.5) leads to $s_{20,w} = 2.1$ S.

From high-speed sedimentation equilibrium experiments at an initial protein concentration of 0.2 mg/mL, $M_r = 338 \pm 7$ kDa and 342 ± 10 kDa are calculated for the native holo- and apo-

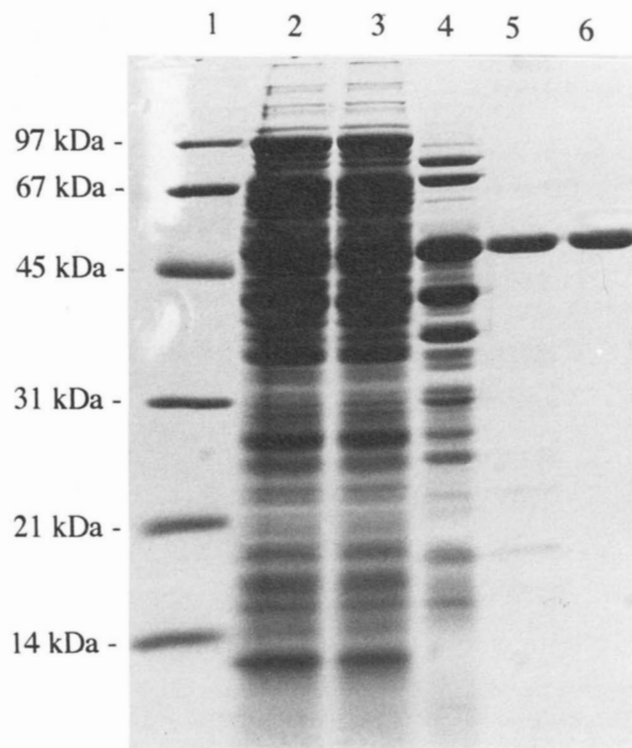


Fig. 1. SDS-PAGE illustrating the purification of enolase from *T. maritima*. Lane 1, molecular mass standards were phosphorylase, 97 kDa; bovine serum albumin, 66 kDa; ovalbumin, 45 kDa; carbonic anhydrase, 31 kDa; trypsin inhibitor, 21.5 kDa; lysozyme, 14 kDa; lane 2, crude extract; lane 3, 35–70% ammonium sulfate precipitate after resuspension and dialysis against low-salt buffer; lanes 4–6, combined fractions of enolase after hydrophobic interaction chromatography, anion-exchange chromatography, and gel-permeation chromatography, respectively. The gel was stained with Coomassie brilliant blue.

enzyme, respectively. In the presence of 4 M GdmCl, dissociation yields $M_r = 55 \pm 6$ kDa, assuming a decrease in the partial specific volume of 5% (Durchschlag & Jaenicke, 1982).

The sedimentation data are confirmed by gel-permeation chromatography and SDS-PAGE: gel filtration under native conditions, in the presence of Mg^{2+} , led to a molecular mass of

Table 1. Purification of enolase from *T. maritima*^a

Fraction	Volume (mL)	Total protein (mg)	Total units (U)	Specific activity (U/mg)	Purification factor	Recovery (%)
Crude extract	90	1,050	5,900	6	1	100
AS-precipitate ^b (40–65%)	80	794	5,870	7	1.3	99
Phenylsepharose	200	62	4,788	77	13	80
Q-Sepharose	70	17	3,910	240	42	66
Superdex 200 pg	16	12	2,875	250	44	49

^a Crude extract was obtained from 100 g of cells. Enolase activity was determined under standard conditions at 40 °C.

^b Ammonium sulfate precipitate, resuspended and dialyzed against low salt buffer.

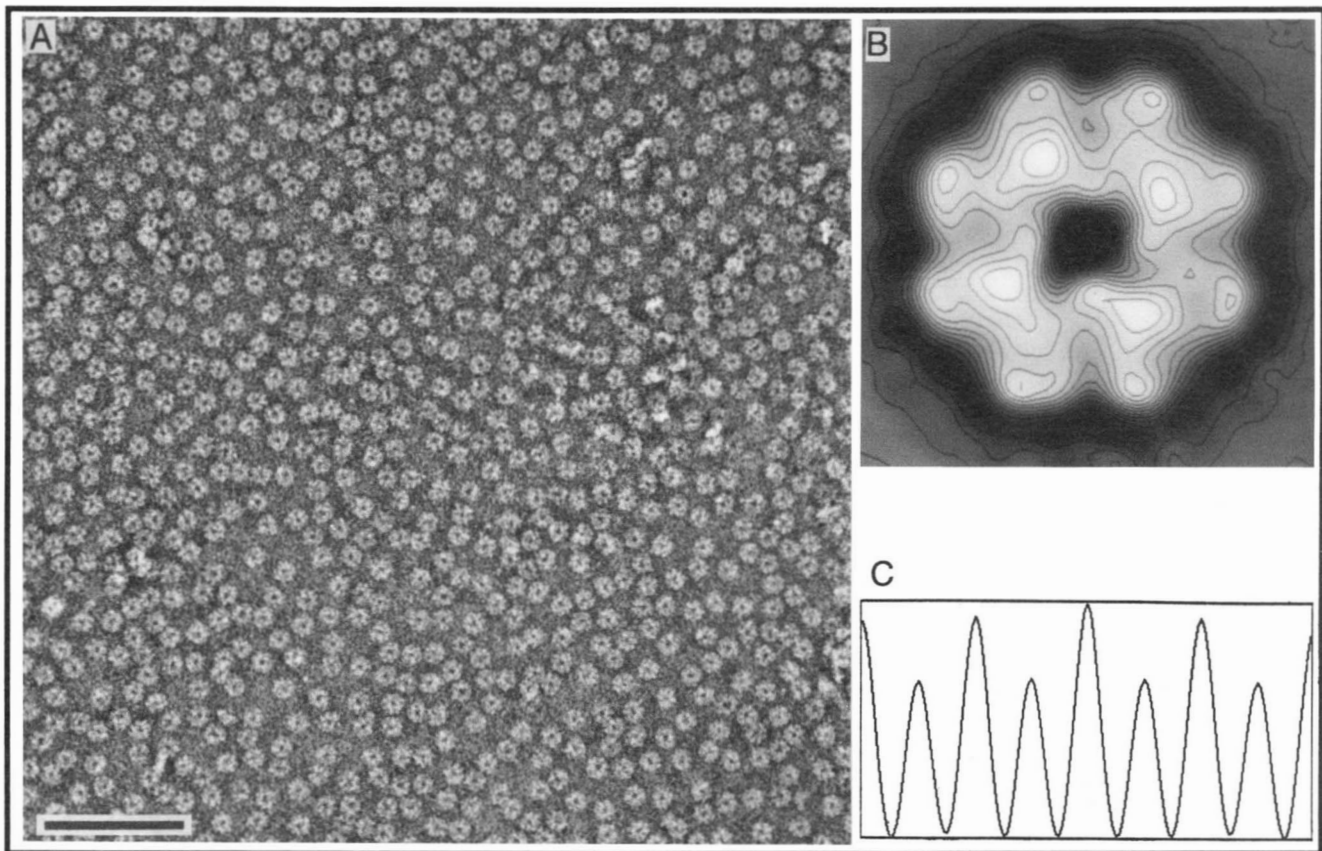


Fig. 3. **A:** Field view of negatively stained (3% uranyl acetate) *T. maritima* enolase. Scale bar: 100 nm. **B:** Average over 779 aligned particles, with contour lines superimposed. Fourfold symmetry was not imposed on the average. **C:** Orientational correlation function of Figure 3B; for details see the Materials and methods.

Stability

The irreversible heat inactivation of enolase was monitored in the temperature range between 60 and 100 °C (Fig. 7). To quantify the effect of Mg²⁺ on the thermal stability, the holoenzyme was incubated for 2 h in 50 mM HEPES buffer in the presence of 5 mM MgCl₂, and the apoenzyme in the presence of 2 mM EDTA. Figure 7 shows that the thermal transition is shifted from 90 °C to 94 °C in the presence of the stabilizing cofactor. Moreover, the thermal transition in the absence of Mg²⁺ becomes significant at 75 °C, whereas in the presence of excess magnesium, the temperature limit of stability is almost 90 °C; at the same time, a slight increase in cooperativity is observed. The high thermal stability is paralleled by an anomalously high stability against denaturants such as GdmCl. Taking the residual activity or fluorescence emission as a measure, the transition midpoints at 20 °C are shifted from 0.5 M GdmCl in the case of rabbit muscle enolase to 3 M GdmCl for the enzyme from *T. maritima*. Comparison of the two unfolding transitions reveals that deactivation precedes denaturation (data not shown).

Discussion

Thermotogales are early descendants from the bacterial branch of the phylogenetic tree. *T. maritima*, with a maximal growth

temperature of 90 °C, is a hyperthermophilic representative of this order (Stetter, 1993).

Previous studies on a number of glycolytic enzymes from *T. maritima* have shown that the protein inventory of the bacterium is intrinsically stable (Rehaber & Jaenicke, 1992; Jaenicke, 1993; Ostendorp et al., 1993). The molecular mechanism responsible for the anomalous stability is still unresolved (Jaenicke, 1991).

As has become clear from systematic investigations of models such as phage T4 lysozyme (Matthews, 1991) and LDH (Jaenicke, 1991), there are three levels in the hierarchy of protein structure that contribute to the intrinsic stability of proteins, local interactions in the hydrophobic core or in secondary-structural elements, interactions between domains or subdomains, and subunit interactions. At the level of local packing, hydrodynamic experiments, X-ray data, and H-D exchange rates have shown that proteins from thermophiles exhibit drastically reduced flexibility (Wrba et al., 1990; Jaenicke, 1993; Korndörfer et al., 1995). The differences vanish with increasing temperature, so that under conditions close to the temperature of optimal growth (90 °C), the H-D exchange rates of *Thermotoga* enzymes come close to the respective data for their mesophilic counterparts at ~30 °C (Wrba et al., 1990; P. Závodszy, unpubl. results). A difference that is obvious from crystallographic data is an increase in surface charges available

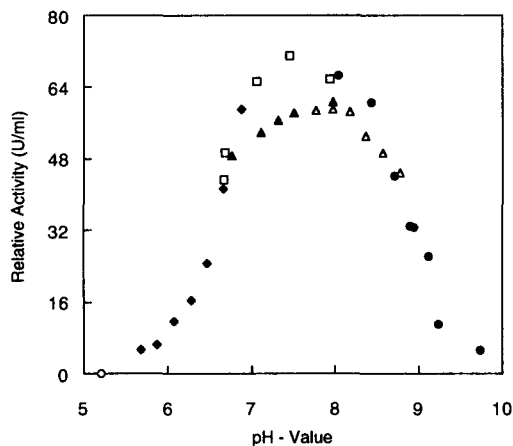


Fig. 4. Effect of pH on the catalytic activity of *T. maritima* enolase. The following buffers were used: ○, NaAc/HAc, pH 4.6–5.2; ◆, imidazole/HCl, pH 5.7–6.8; □, Tris/HCl, pH 6.7–8.0; ▲, HEPES/NaOH, pH 6.8–8.0; △, Tricine, pH 7.8–8.7; ●, boric acid/NaOH, pH 8.6–10.6. All buffers were 50 mM and titrated with NaCl to an ionic strength of 0.1 at the desired pH. Measurements are under standard conditions at 40 °C.

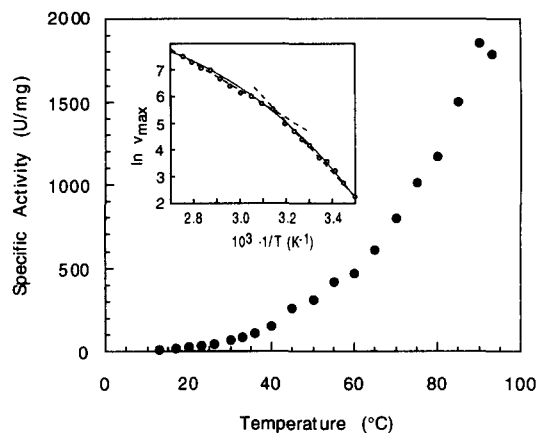


Fig. 6. Temperature dependence of the specific activity of *T. maritima* enolase. Dehydration of 2-PGA was measured in Tris/HCl buffer titrated to pH 7.5 at the indicated temperature. Concentrations of Mg^{2+} were adapted to the different temperatures, according to the measured K_m values and regarding the inhibitory effect of magnesium at higher concentrations (10 mM Mg^{2+} at 13–25 °C, 5 mM Mg^{2+} at 26–45 °C, 1 mM Mg^{2+} at 50–65 °C, and 0.5 mM Mg^{2+} at 70–95 °C). **Inset:** Arrhenius plot for the dehydration of 2-PGA.

for ion-pair formation (Korndörfer et al., 1994). In the case of GAPDH, they are mainly exposed to the solvent, without affecting the subunit interactions in a significant way. In contrast, in the case of LDH, the state of association is clearly correlated with the stability of the enzyme: both proteolytic degradation and thermal denaturation show that the stability is gradually decreased in proceeding from the native tetramer via the “proteolytic dimer” (Opitz et al., 1987) to the monomeric folding intermediate on the sequential pathway of reconstitution (Girg

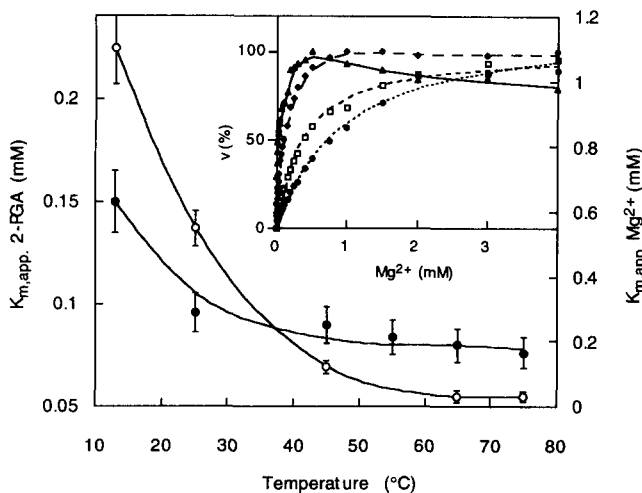


Fig. 5. Effect of temperature on the apparent K_m values for the substrate, 2-PGA, and the cofactor, Mg^{2+} , of *T. maritima* enolase. Filled circles represent measurements with 2-PGA, open circles with Mg^{2+} . Data points were derived as described in the Materials and methods. Error bars indicate the standard estimate of errors. **Inset:** Mg^{2+} dependence of the reaction rate of enolase at 4 different temperatures: ···●···, 13 °C; ---□---, 25 °C; —◆—, 45 °C; —▲—, 65 °C. Maximum velocity at each temperature is set to 100%.

et al., 1981). Considering the stability of folding intermediates, it is remarkable that in the case of GAPDH the low-temperature intermediate of the mesophilic yeast enzyme is the structured monomer (Bartholmes & Jaenicke, 1975), whereas in the case of the *T. maritima* enzyme, it is the native-like tetramer (Schultes & Jaenicke, 1991). Obviously, in these cases the shift to higher assemblies contributes to stability.

In the given context, it is tempting to ascribe the high intrinsic stability of *Thermotoga* enolase to its anomalous quaternary structure, because homologs from mesophilic eukaryotic sources are known to be dimeric (Wold, 1971). However, two findings contradict this hypothesis. First, there are reports of nonthermophilic octamers in the literature, which suggest that this state of association is a characteristic of bacterial enolases rather than enolases with anomalous thermal stability: both the enzyme

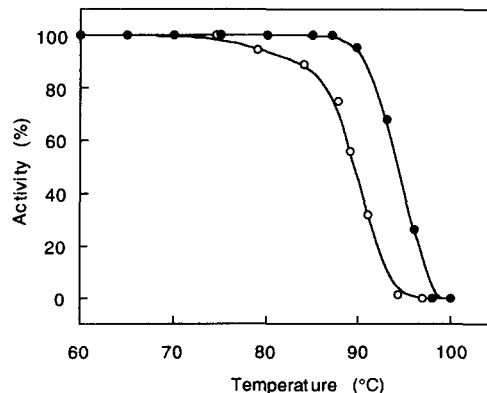


Fig. 7. Thermal stability of enolase from *T. maritima*. Stability of enolase was measured after a 2-h incubation in 50 mM HEPES buffer, pH 7.5, in the presence of 2 mM EDTA for the apoenzyme (○) and in the presence of 5 mM $MgCl_2$ for the holoenzyme (●).

from *Bacillus megaterium* (Singh & Setlow, 1978) and *Streptococcus mutans* (Kaufmann & Bartholmes, 1992) exhibit native and subunit molecular masses of ca. 345 and 44 kDa, respectively. Second, in a recent study, Peak et al. (1994) have reported that enolase from the hyperthermophilic archaeon *P. furiosus* seems to be a homodimer. Thus, the hyperthermophilic nature of the *Thermotoga* enzyme cannot be attributed to its anomalous state of association.

As has been frequently observed, the substrate 2-PGA, and/or the cofactor Mg^{2+} , enhance the stability (Fig. 7). On the other hand, excess Mg^{2+} causes inhibition of the catalytic activity. This effect has also been reported for mesophilic enolases, where it has been discussed in terms of additional binding sites for inhibitory metal ions (Faller et al., 1977; Lee & Nowak, 1992).

The K_m values for the cofactor and the substrate exhibit a pronounced temperature dependence (Fig. 5). However, at physiological temperature, both reach plateau values close to the level observed for the mesophilic enzyme at room temperature. "Corresponding states" of homologous enzymes under their respective physiological conditions have often been observed for organisms belonging to different climatic zones (Hochachka & Somero, 1973; Somero, 1978; Jaenicke, 1993). As has been found for other *Thermotoga* enzymes (e.g., GAPDH and LDH), the leveling of K_m at high temperature cannot be generalized (Hecht et al., 1989; Wrba et al., 1990). Evidently, the simultaneous optimization with respect to folding, catalysis, regulation, and turnover sometimes requires compromises with respect to one or another property. In this connection, enolase from *T. maritima* has been most successful in its multifunctional adaptation, showing maximum catalytic efficiency and stability at the upper limit of the physiological temperature regime. At the optimal temperature, the specific activity reaches ~2,000 U/mg. Corresponding values for the mesophilic homologs are ~70 U/mg for the enzyme from *B. megaterium* (Singh & Setlow, 1978), ~160 U/mg for *Escherichia coli* (Spring & Wold, 1975), and 450–900 U/mg for *Thermus aquaticus* (Stellwagen et al., 1973).

The temperature dependence of the activity of the enzyme shows nonlinear behavior (Fig. 6). Apparently, the change in the activation energy correlates with the temperature range, where the apparent K_m values for 2-PGA and Mg^{2+} reach their constant plateau value ($\geq 45^\circ C$). A similar behavior has been reported for LDH from *Thermus thermophilus* (Lakatos et al., 1978), as well as for the GAPDH from *Thermoproteus tenax* (Hensel et al., 1987), *Methanothermobacter fervidus* (Fabry & Hensel, 1987), and *T. maritima* (Wrba et al., 1990). The pH dependence of the catalytic activity also confirms data reported for other enolases (Wold, 1971; Stellwagen et al., 1973). Similarly, the inhibition by the magnesium-fluoride-phosphate complex is a common property of all enolases investigated so far (Kaufmann & Bartholmes, 1992). The molecular explanation of the synergism has recently been given, based on the crystal structure of the enolase- Mg^{2+} - F^- - P_i quaternary complex from yeast (Lebioda et al., 1993).

Making use of electron microscopy, insight into the topology of the native quaternary structure can be obtained. Apart from the size of the molecule, three conclusions can be drawn: (1) The enzyme is homogeneous, with the ring-shaped octamer as the predominant species. (2) Because only end-on views are observed, the enzyme must be a disk; its diameter is 17 nm. (3) Image processing clearly brings out fourfold symmetry of the

particles proving the subunit stoichiometry to be a tetramer of dimers (Fig. 3A,B,C). This quaternary structure has also been reported for the enzyme from *T. aquaticus*; however, in this case the data were interpreted in terms of a "prolate ellipsoid with an axial ratio of 4, suggesting that the eight polypeptide chains form a cubic array of eight globular subunits" (Stellwagen et al., 1973, p. 1558). Obviously, the previously mentioned dimensions and the results of the image processing contradict this model. Considering at this point the frictional properties of the *Thermotoga* enzyme, the sedimentation analysis yields $f/f_0 = 1.403$, corresponding to an oblate shape with an axial ratio of ~9. Upon denaturation, the quaternary structure shows different behavior depending on the solvent conditions: at pH 2, the 7 S particle clearly indicates a compact intermediate, whereas at high GdmCl concentration, the low s -value (2 S) must belong to the monomer in its fully denaturated state. Addition of the cofactor Mg^{2+} leads to a 5% decrease in sedimentation velocity. Whether this effect is caused by some kind of subunit rearrangement or alterations in solvation as a consequence of ion binding needs further analysis.

Materials and methods

Materials

Phenyl-Sepharose FF (high sub), Q-Sepharose HP, and a Superdex 200 pg-column (XK 16/60) were purchased from Pharmacia (Uppsala).

2-PGA, PEP, NADH, and DNaseI were purchased from Boehringer (Mannheim). The concentration of stock solutions of 2-PGA were measured by monitoring the oxidation of NADH spectrophotometrically using rabbit muscle enolase, pyruvate kinase, and LDH (Lamprecht & Heinz, 1984). All proteins were purchased from Boehringer (Mannheim). Ultra-pure GdmCl and trypsin were products of Schwarz-Mann (Orangeburg, New York) and Worthington (Washington), respectively. HEPES was from Fluka (Buchs). All other chemicals were analytical-grade substances from Merck (Darmstadt). Quartz-bidistilled water was used throughout. Buffer solutions were filtered and carefully degassed.

Growth of *T. maritima*

A culture of *T. maritima* (MSB 8; DSM 3109) was kindly provided by Drs. K.O. Stetter and R. Huber (Lehrstuhl für Mikrobiologie, Universität Regensburg). Cells were grown according to Huber et al. (1986). Large-scale cultures were grown in a 300-L enamel-protected fermentor at $80^\circ C$ under N_2 (2.5 L/min), with gentle stirring (100 rpm). Cells were harvested in a Padberg centrifuge and stored at $-70^\circ C$. Up to 200 g wet cell material per 300-L culture were obtained.

Purification of enolase

All purification steps were performed at room temperature. Unless noticed otherwise, 50 mM Tris/HCl buffer, pH 7.5, with 5 mM $MgCl_2$ and 1 mM EDTA (buffer A), was used as solvent.

Crude extract

Frozen cells (100 g wet weight) were thawed, resuspended in 250 mL buffer A, and passed through a French press ([1.0–1.4] ×

10^8 N/m^2 , i.e., 15–20,000 psi); after the addition of $15 \mu\text{g/mL}$ DNaseI, the suspension was incubated at 37°C for 45 min. Insoluble material was removed by centrifugation (2 h at $48,000 \times g$). The pellet was resuspended in buffer A, centrifuged again (1 h at $48,000 \times g$), and the supernatants were pooled.

Ammonium sulfate precipitation

Solid ammonium sulfate was added to the crude extract in portions of 20 g/h, under continuous stirring up to 35% saturation. The suspension was further stirred for 1 h. Following centrifugation (2 h at $48,000 \times g$), ammonium sulfate was added to bring the supernatant to 70% saturation. After spinning down precipitated proteins (2 h at $48,000 \times g$), the pellet was dissolved in buffer A, 30% saturated with ammonium sulfate.

Hydrophobic chromatography

The resolved 35–70% ammonium sulfate pellet was applied to a 160-mL phenyl-Sepharose FF (high sub) column ($5.0 \times 8 \text{ cm}$), equilibrated with buffer A plus 30% saturated ammonium sulfate. Enolase activity was eluted applying a linear 30 → 0% ammonium sulfate gradient in a total volume of 2 L. Active fractions were pooled and dialyzed against buffer A.

Ion-exchange chromatography

The dialyzed solution was applied to a 70-mL Q-Sepharose HP column ($2.6 \times 13 \text{ cm}$) equilibrated with buffer A. Enolase activity was eluted using a linear 0 → 1.0 M NaCl gradient contained in 10 column volumes.

Gel-permeation chromatography

The collected active fractions were concentrated in an Amicon ultrafiltration cell (50 mL) using a PM-30 membrane up to a concentration of about 10 mg/mL ; 1.5 mL of this solution were applied to a 120-mL Superdex 200-pg column ($1.6 \times 60 \text{ cm}$). The column was equilibrated with buffer A with 100 mM NaCl at a flow rate of 1 mL/min. The purified enzyme was pooled in 1-mL fractions containing 30% glycerol and stored at -20°C .

Enzyme assays

The catalytic activity of *T. maritima* enolase was measured by monitoring the formation of PEP spectrophotometrically at 240 nm, as first suggested by Warburg and Christian (1941). One unit of enzyme activity is defined as the amount of enzyme catalyzing the formation of $1 \mu\text{mol}$ substrate in 1 min. Because the extinction coefficient of PEP varies with pH, Mg^{2+} concentration (Wold & Ballou, 1957), and temperature (Stellwagen et al., 1973), the results were analyzed using values of ϵ determined at the respective conditions.

Assays were performed in 1-cm quartz cuvettes sealed with silicone stoppers in a Perkin-Elmer 551S spectrophotometer with a thermostated cell holder. Temperature was monitored using a digital thermometer 865 (Keithley, Cleveland, Ohio) with an encapsulated thermistor.

The standard assay mixture contained 2 mM Mg^{2+} and 2 mM 2-PGA in 50 mM Tris/HCl buffer, pH 7.5. Unless stated otherwise, enolase activity was measured at 40°C using an extinction coefficient for PEP of $1.34 \times 10^{-3} \mu\text{M}^{-1} \text{ cm}^{-1}$. The pH of the buffer solutions was adjusted at 20°C for the desired temperature, making use of published $\Delta\text{pH}/^\circ\text{C}$ temperature coefficients.

Kinetic measurements

The ionic strength of the buffers used for pH-dependent activity measurements was adjusted to 0.1 M using NaCl. The kinetic parameters, V_{max} and K_m , were obtained (1) from an unweighted least-squares analysis of plots of $[S_0]/v_0$ versus v_0 (Hanes plot), with v_0 as initial velocity and $[S_0]$ as initial substrate concentration and, (2) from weighted least-square fits to a hyperbola. Inhibitor constants were derived from double-reciprocal plots after replotting apparent K_m/V_{max} (slope) and $1/V_{max}$ (intercept) against the concentration of the inhibitor (Henderson, 1992).

Protein determination

The extinction coefficient of enolase was determined using the BCA protein assay (Pierce, Rockford, Illinois), following the procedure recommended by the manufacturer, with bovine serum albumin as standard.

Enzyme stability

In order to investigate the long-term stability of the enzyme at high temperature, 200- μL portions of the enzyme solution were filled in 0.5-mL safe-lock microtubes (Eppendorf, Hamburg) at protein concentrations of about $10 \mu\text{g/mL}$ and overlaid with Nujol mineral oil (Perkin Elmer, Überlingen). After incubation at the desired temperature for 2 h, samples were cooled rapidly and assayed immediately for residual activity.

The stability against denaturants was determined in aliquots incubated for at least 48 h at 20°C and protein concentrations of 10–16 $\mu\text{g/mL}$. In order to exclude reactivation during the standard assay, 20 $\mu\text{g/mL}$ trypsin was added in all stability and reconstitution experiments (Chan et al., 1973).

Determination of molecular masses

A Superdex 200 HR 10/30 column ($1.0 \times 30 \text{ cm}$) was used to determine the molecular weight of the native protein; 50 mM Tris/HCl buffer, pH 7.5, with 1 mM EDTA, 5 mM MgCl_2 , and 300 mM NaCl was applied as eluent. Marker proteins: (1) thyroglobulin, 670 kDa; (2) apoferritin, 450 kDa; (3) catalase, 232 kDa; (4) aldolase, 158 kDa; (5) immunoglobulin G, 150 kDa; (6) enolase from rabbit muscle, 88 kDa; (7) bovine serum albumin, 67 kDa; (8) ovalbumin, 43 kDa; (9) chymotrypsinogen, 25 kDa; (10) cytochrome *c*, 12 kDa. PAGE was carried out using 12% (w/v) acrylamide in standard gels and 5–25% (w/v) acrylamide in gradient gels (See & Jackowski, 1989). Molecular markers were used as described in Figure 1. Gels were stained using silver or Coomassie brilliant blue (Dunn, 1989).

Sedimentation velocity and sedimentation equilibrium measurements were performed in a Beckman model E ultracentrifuge equipped with a high-sensitivity light source and photoelectric scanning system, making use of double sector cells (12 mm) with sapphire windows in an An-G rotor. In order to detect possible concentration-dependent dissociation, the meniscus-depletion technique (Yphantis, 1964) was applied. Scanning wavelengths were 235 and 280 nm, respectively. *s*-Values were determined at 16,000 and 44,000 rev/min, plotting $\ln r$ versus time, and correcting for 20°C and water viscosity. Sedimentation equilibria at 8,000 rev/min were calculated from $\ln c$ versus r^2 plots, mak-

ing use of a computer program developed by Dr. G. Böhm (University of Regensburg). The partial specific volume was assumed to be $0.735 \text{ cm}^3 \text{ g}^{-1}$.

The isoelectric point was determined by isoelectric focusing using IEF gels in a Phast-System (Pharmacia, Uppsala).

Spectral measurements

The magnesium content was measured by atomic absorption spectrometry on a Varian SpectrAA 40. Tightly bound magnesium was removed by extensive dialysis against EDTA (5 mM). Ultraviolet absorption spectra were recorded in Cary 1 and Perkin-Elmer Lambda 5 double-beam spectrophotometers, and fluorescence emission spectra in a Spex Fluoromax™ spectrofluorometer. The excitation wavelength was 280 nm.

Electron microscopy and image processing

A purified sample of the enzyme was applied to a carbon-coated grid, washed once with bidistilled water, and negatively stained with 3% uranyl acetate. Images were taken at 100 kV and a magnification of 45,000 \times in a Philips CM 12 equipped with a Gatan 673 TV system and a Tietz computer for a continuous control of focus and astigmatism (Koster et al., 1989). For image processing, negatives were digitized on an Eikonics 412 CCD camera with pixel size of 0.3 nm. Alignment of the particles, averaging, and classification were performed essentially as described (Schmidt et al., 1994) using the EM program system (Hegerl & Altbauer, 1982). The digitized image was high- and low-pass-filtered; 779 particles were extracted, aligned with cross-correlation and rotational correlation functions, and finally averaged. The aligned particles were also subjected to multivariate statistical analysis and classification (van Heel & Frank, 1981) in order to test whether different kinds of particles were present in the data set.

Amino-terminal sequencing

Determination of N-terminal sequences was performed by Dr. R. Deutzmann (University of Regensburg) using an Applied Biosystems Sequencer 120A/477A.

Acknowledgments

We thank Drs. K.O. Stetter and R. Huber for providing us with *T. maritima* MSB8 cells, and E. Kapfberger and M. Angler (Siemens, Regensburg) for performing the atomic absorption spectroscopy. The help of and discussion with N. Beaucamp and R. Ostendorp are gratefully acknowledged. We thank Dr. W. Baumeister for use of the digitizing facilities at the MPI für Biochemie, Martinsried. This research was supported by grants from the Deutsche Forschungsgemeinschaft (SFB4 (F5), Ja 78/34).

References

- Barnes LD, Stellwagen E. 1973. Enolase from the thermophile *Thermus X-1*. *Biochemistry* 12:1559–1565.
- Bartholmes P, Jaenicke R. 1975. Molecular properties of yeast GAPDH in the presence of ATP and KCl. *Biochem Biophys Res Commun* 64:485–492.
- Blamey JM, Adams MWW. 1994. Characterization of an ancestral type of pyruvate ferredoxin oxidoreductase from the hyperthermophilic bacterium, *Thermotoga maritima*. *Biochemistry* 33:1000–1007.
- Brewer JM. 1981. Yeast-enolase: Mechanism of activation by metal ions. *CRC Crit Rev Biochem* 11:209–254.
- Chan WWC, Mort JS, Chong DKK, MacDonald PDM. 1973. Studies on protein subunits. *J Biol Chem* 248:2778–2784.
- Dunn MJ. 1989. Determination of total protein concentration. In: Harris ELV, Angal S, eds. *Protein purification methods, a practical approach*. Oxford, UK: IRL Press at Oxford University Press. pp 10–37.
- Durchschlag H, Jaenicke R. 1982. Partial specific volume changes of proteins: Densimetric studies. *Biochem Biophys Res Commun* 108:1074–1079.
- Fabry S, Hensel R. 1987. Purification and characterization of D-GAPDH from the thermophilic archaeobacterium *Methanothermobacter fervidus*. *Eur J Biochem* 165:147–155.
- Faller LD, Baroudy BM, Johnson AM, Ewall RX. 1977. Magnesium ion requirements for yeast enolase activity. *Biochemistry* 16:3864–3869.
- Farber GK, Petsko GA. 1990. The evolution of α/β barrel enzymes. *Trends Biochem Sci* 15:228–234.
- Girg R, Rudolph R, Jaenicke R. 1981. Limited proteolysis of porcine-muscle lactate dehydrogenase by thermolysin during reconstitution yields dimers. *Eur J Biochem* 119:301–305.
- Hecht K, Wrba A, Jaenicke R. 1989. Catalytic properties of thermophilic LDH and halophilic MDH at high temperature and low water activity. *Eur J Biochem* 183:69–74.
- Hegerl R, Altbauer A. 1982. The electron microscopy program system. *Ultra-microscopy* 9:109–116.
- Henderson PJF. 1992. Statistical analysis of enzyme kinetic data. In: Eisen-thal R, Danson MJ, eds. *Enzyme assay, a practical approach*. Oxford, UK: IRL Press at Oxford University Press. pp 277–316.
- Hensel R, Laumann S, Lang J, Heumann H, Lottspeich F. 1987. Characterization of two D-GAPDHs from the extremely thermophilic archaeobacterium *Thermoproteus tenax*. *Eur J Biochem* 170:325–333.
- Hochachka PW, Somero GN. 1973. *Strategies of biochemical adaptation*. Philadelphia, Pennsylvania: Saunders.
- Holland MJ, Holland JP, Thill GP, Jackson KA. 1981. The primary structures of two yeast enolase genes. *J Biol Chem* 256:1385–1395.
- Huber R, Langworthy TA, König H, Thomm M, Woese CR, Sleytr UB, Stetter KO. 1986. *Thermotoga maritima* sp. nov. represents a new genus of unique extremely thermophilic eubacteria growing up to 90°C. *Arch Microbiol* 144:324–333.
- Jaenicke R. 1991. Protein stability and molecular adaptation to extreme conditions. *Eur J Biochem* 202:715–728.
- Jaenicke R. 1993. Structure–function relationship of hyperthermophilic enzymes. In: Himmel ME, Georgiou G, eds. *Biocatalyst design for stability and specificity*. ACS Symposium Series No. 516:53–67.
- Kaghad M, Dumont X, Chalou P, Lelias JM, Lamandé N, Lucas M, Lazar M, Caput D. 1990. Nucleotide sequences of cDNAs α and γ enolase mRNAs from mouse brain. *Nucleic Acids Res* 18:3638.
- Kaufmann M, Bartholmes P. 1992. Purification, characterization and inhibition by fluoride of enolase from *Streptococcus mutans* DSM 320523. *Caries Res* 26:110–116.
- Korndörfer I, Steipe B, Huber R, Tomschy A, Jaenicke R. 1995. The crystal structure of holo-GAPDH from the hyperthermophilic bacterium *Thermotoga maritima* at 2.5 Å resolution. *J Mol Biol*. Forthcoming.
- Koster AJ, de Ruijter WJ, van den Bos A, van der Mast KD. 1989. Autotuning of a TEM using minimum electron dose. *Ultramicroscopy* 27:251–272.
- Lakatos S, Halász G, Závodszy P. 1978. Conformational stability of lactate dehydrogenase from bacillus *Thermus aquaticus*. *Biochem Soc Trans* 6:1195–1197.
- Lamprecht W, Heinz F. 1984. D-Glycerate 2-phosphate and phosphoenolpyruvate. In: Bergmeyer HU, ed. *Methods of enzymatic analysis, vol 6*. Weinheim/Deerfield Beach: Verlag Chemie. pp 342–350.
- Lebioda L, Zhang E, Lewinski K, Brewer JM. 1993. Fluoride inhibition of yeast enolase: Crystal structure of the enolase-Mg²⁺-F⁻-P_i complex at 2.6 Å. *Proteins Struct Funct Genet* 16:219–225.
- Lee BH, Nowak T. 1992. Metal ion specificity at the catalytic site of yeast enolase. *Biochemistry* 31:2172–2180.
- Matthews BM. 1991. Mutational analysis of protein stability. *Curr Opin Struct Biol* 1:17–21.
- Opitz U, Rudolph R, Jaenicke R, Ericsson L, Neurath H. 1987. Proteolytic dimers of porcine muscle lactate dehydrogenase: Characterization, folding, and reconstitution of the truncated and nicked polypeptide chain. *Biochemistry* 26:1399–1406.
- Ostendorp R, Liebl W, Schurig H, Jaenicke R. 1993. The L-LDH gene of the hyperthermophilic bacterium *Thermotoga maritima* cloned by complementation in *Escherichia coli*. *Eur J Biochem* 216:709–715.
- Peak MJ, Peak JG, Stevens FJ, Blamey J, Mai X, Zhou ZH, Adams MWW. 1994. The hyperthermophilic glycolytic enzyme enolase in the archaeon, *Pyrococcus furiosus*: Comparison with mesophilic enolases. *Arch Biochem Biophys* 313:280–286.

- Penczek P, Radermacher M, Frank J. 1992. Three-dimensional reconstruction of single particles embedded in ice. *Ultramicroscopy* 40:33-53.
- Rehaber V, Jaenicke R. 1992. Stability and reconstitution of D-glyceraldehyde-3-phosphate dehydrogenase from the hyperthermophilic eubacterium *Thermotoga maritima*. *J Biol Chem* 267:10999-11006.
- Schmidt M, Rutkat K, Rachel R, Pfeifer G, Jaenicke R, Viitanen P, Lorimer G, Buchner J. 1994. Symmetric complexes of GroE chaperonins as part of the functional cycle. *Science* 265:656-659.
- Schultes V, Jaenicke R. 1991. Folding intermediates of hyperthermophilic D-glyceraldehyde-3-phosphate dehydrogenase from *Thermotoga maritima* are trapped at low temperature. *FEBS Lett* 290:235-238.
- Schurig H, Beaucamp N, Ostendorp R, Jaenicke R, Adler E, Knowles JR. 1995. Phosphoglycerate kinase and triosephosphate isomerase from the hyperthermophilic bacterium *Thermotoga maritima* form a covalent bifunctional enzyme complex. *EMBO J* 14:442-451.
- See YP, Jackowski G. 1989. Estimating molecular weights of polypeptides by SDS gel electrophoresis. In: Creighton TE, ed. *Protein structure, a practical approach*. Oxford, UK: IRL Press at Oxford University Press. pp 1-19.
- Singh RP, Setlow P. 1978. Enolase from spores and cells of *Bacillus megaterium*: Two-step purification of the enzyme and some of its properties. *J Bacteriol* 134:353-355.
- Somero GN. 1978. Temperature adaptation of enzymes: Biological optimization through structure-function compromises. *Annu Rev Ecol Syst* 9:1-29.
- Spring GT, Wold D. 1975. Enolase from *Escherichia coli*. *Methods Enzymol* 42:323-329.
- Stec B, Lebiada L. 1990. Refined structure of yeast apo-enolase at 2.25 Å resolution. *J Mol Biol* 211:235-248.
- Stellwagen E, Cronlund MM, Barnes LD. 1973. A thermostable enolase from the extreme thermophile *Thermus aquaticus* YT-1. *Biochemistry* 12:1552-1559.
- Stetter KO. 1993. The lesson of archaeobacteria. In: Bengtson S, ed. *Early life on earth*. Nobel Symposium 84. New York: Columbia University Press. pp 101-109.
- van Heel M, Frank J. 1981. Use of multivariate statistics in analysing the images of biological macromolecules. *Ultramicroscopy* 6:187-194.
- Warburg O, Christian W. 1941. Isolierung und Kristallisation des Gärungsferments Enolase. *Biochem Z* 310:384-390.
- Weng M, Makaroff CA, Zalkin H. 1986. Nucleotide sequence of *Escherichia coli pyrG* encoding CTP synthetase. *J Biol Chem* 261:5568-5574.
- Wold F. 1971. Enolase. In: PD Boyer, ed. *The enzymes, 3rd ed, vol 5*. New York: Academic Press. pp 499-538.
- Wold F, Ballou CE. 1957. Studies on the enzyme enolase. I. Equilibrium studies. *J Biol Chem* 227:301-312.
- Wrba A, Schweiger A, Schultes V, Jaenicke R, Závodszky P. 1990. Extremely thermostable D-glyceraldehyde-3-phosphate dehydrogenase from the eubacterium *Thermotoga maritima*. *Biochemistry* 29:7584-7592.
- Yphantis DA. 1964. Equilibrium ultracentrifugation of dilute solutions. *Biochemistry* 3:297-317.